

PERSPECTIVE • OPEN ACCESS

Human activities now fuel two-thirds of global methane emissions

To cite this article: R B Jackson *et al* 2024 *Environ. Res. Lett.* **19** 101002

View the [article online](#) for updates and enhancements.

You may also like

- [Land-use change as a major driver for mid-20th-century flood intensity reduction in the Southeastern US](#)
Zhixiong Shen, Nicholas Conway, Shaowu Bao *et al.*
- [Temporal and spatial changes in the environmental lapse rate distribution over the Arctic](#)
Zelu Zhang, Jonathan Bamber and Adam Igneczi
- [Assessing GEDI data fusions to map woodpecker distributions and biodiversity hotspots](#)
Lisa H Elliott, Jody C Vogeler, Joseph D Holbrook *et al.*

UNITED THROUGH SCIENCE & TECHNOLOGY



The Electrochemical Society
Advancing solid state & electrochemical science & technology

248th ECS Meeting

Chicago, IL
October 12-16, 2025
Hilton Chicago



Science + Technology + YOU!

Register by
September 22
to **save \$\$**

REGISTER NOW

ENVIRONMENTAL RESEARCH
LETTERS

PERSPECTIVE

Human activities now fuel two-thirds of global methane emissions

R B Jackson^{1,2,*}, M Saunois³, A Martinez³, J G Canadell⁴, X Yu¹, M Li¹, B Poulter⁵,
P A Raymond⁶, P Regnier⁷, P Ciais³, S J Davis¹ and P K Patra^{8,9}¹ Department of Earth System Science, Stanford University, Stanford, CA 94305-2210, United States of America² Woods Institute for the Environment and Precourt Institute for Energy, Stanford University, Stanford, CA 94305-2210, United States of America³ Laboratoire des Sciences du Climat et de l'Environnement, LSCE-IPSL (CEA-CNRS-UVSQ), Université Paris-Saclay, 91191 Gif-sur-Yvette, France⁴ Global Carbon Project, CSIRO Environment, Canberra ACT 2601, Australia⁵ Biospheric Sciences Laboratory, NASA Goddard Space Flight Center, Greenbelt, MD 20771, United States of America⁶ Yale School of the Environment, Yale University, New Haven, CT 06511, United States of America⁷ Department Geoscience, Environment & Society, Université Libre de Bruxelles, 1050 Brussels, Belgium⁸ Research Institute for Global Change, JAMSTEC, 3173-25 Showa-machi, Kanazawa, Yokohama 236-0001, Japan⁹ Research Institute for Humanity and Nature, 457-4 Motoyama, Kamigamo, Kyoto 6038047, Japan

* Author to whom any correspondence should be addressed.

E-mail: rob.jackson@stanford.edu**Keywords:** methane, climate change, wetlands, agriculture, fossil fuels and energy

OPEN ACCESS

RECEIVED
30 May 2024REVISED
2 July 2024ACCEPTED FOR PUBLICATION
17 July 2024PUBLISHED
10 September 2024Original content from
this work may be used
under the terms of the
[Creative Commons
Attribution 4.0 licence](#).Any further distribution
of this work must
maintain attribution to
the author(s) and the title
of the work, journal
citation and DOI.

Global average surface temperatures shattered all-time records in 2023 at 1.45 ± 0.12 °C above pre-industrial levels (WMO 2024). Worsened by climate change-induced drought, Canadian wildfires burned 18.5 million hectares, nearly three-times more land area than in any previous year on record (NRC 2023). Parts of the Amazon River reached their lowest levels in 120 years of data-keeping and, in places, recorded surface water temperatures near 40 °C (Rodrigues 2023). The world has reached the threshold of a 1.5 °C increase in global average surface temperature and is only beginning to experience the full consequences.

Methane (CH₄) is the second most important anthropogenic greenhouse gas after carbon dioxide. It contributed 0.5 °C of warming in the 2010s relative to the late 1800s—two-thirds as much warming as CO₂ (IPCC 2021). It is also far more potent than CO₂ ton for ton, with a global warming potential (GWP) >80 and 30 times more than CO₂ for the first twenty years and century after release, respectively (Forster *et al* 2021).

Methane is rising faster in relative terms than any major greenhouse gas and is now 2.6-fold higher than in pre-industrial times. Global average methane concentrations reached 1931 parts per billion (ppb) in January of 2024 (Lan *et al* 2024). Annual increases in methane are also accelerating for reasons that are debated. Global methane concentrations rose by 15, 18, 13, and 10 ppb each year from 2020 through 2023, respectively, the second, first, fourth, and fourteenth largest increases since the U.S. National Oceanic and

Atmospheric Administration (NOAA) methane time series began in 1983 (Lan *et al* 2024).

The Global Carbon Project updates its Global Methane Budget (GMB) every few years (Saunois *et al* 2016, 2020, 2024). The GMB integrates results of: (1) bottom-up (BU) estimates based on process-based models for estimating wetland surface emissions and atmospheric chemistry, inventories of anthropogenic emissions, and data-driven extrapolations, and (2) top-down (TD) CH₄ emission estimates based on atmospheric observations and an inverse-modeling framework. Here, we summarize new estimates of the GMB based on the new GMB (Saunois *et al* 2024). We estimate CH₄ sources and sinks for the periods 2000–2002 and 2018–2020, as well as for the most-recent year (2020), the last year that full global TD and BU methane datasets are available. We compare 3 year-average estimates to smooth the inter-annual variability signals from climatic variability such as the El Niño–Southern Oscillation (ENSO) that influence natural emissions from wetlands and other ecosystems, as well as from the chemical sink.

We provide insights on data for methane sources and sinks globally and for the geographical regions and economic sectors whose emissions have changed the most since 2000. We also provide additional data on changes in recent years using satellite-based inversions using the TROPospheric Monitoring Instrument (TROPOMI) (e.g. Yu *et al* 2023).

1. Methods

Our methods and data are derived from the Global Carbon Project's most recent global methane budget (Saunio *et al* 2024). We employ a TD ensemble of 24 inversions based on seven different inverse systems that use data for atmospheric CH₄ concentrations to constrain total emissions and attribute them to primary sources. The TD inversions are either constrained by surface observations for the period 2000–2020 (18 out of 24 simulations), or satellite observations from the Greenhouse Gases Observing Satellite (GOSAT) for the period 2010–2020. Prior fluxes, observations, treatments, and optimization configurations varied modestly across the inversions as described in Saunio *et al* (2024).

Most of the atmospheric inversions used the same OH field, treated as constant over time, attributing changes in methane concentrations to altered emissions rather than to altered atmospheric oxidative capacity. Although, chemistry-climate models suggest potential OH increases between 2000 and 2010 and decreases after 2010 (e.g. Zhao *et al* 2020, Skeie *et al* 2023), OH inferred from hydrofluorocarbon and methyl chloroform observations suggest insignificant trends over the past two decades (Patra *et al* 2021, Thompson *et al* 2024). Models and observations also indicate small interannual variability of OH (<2% in Thompson *et al* (2024) and Patra *et al* (2021)), implying ~ 10 – 11 Tg yr⁻¹ uncertainty in interannual flux variability if OH variability is ignored in recent decades (Saunio *et al* 2024). In 2020, OH seems to have decreased sharply by 2% compared to 2019 attributable to reduced NO_x emissions that may have explained at least half of the surge in growth rate (Peng *et al* 2022). In future scenarios, while decarbonization can decrease methane emissions, the associated reduction in NO_x emissions has the potential to increase methane's lifetime in the atmosphere. The overall climate and air quality benefits thus require careful evaluation.

The Global Methane Budget also employs detailed BU accounting that includes global inventories and biogeochemical modeling that provides a more detailed attribution to sources but lacks the constraint of total atmospheric growth rate used in TD approaches. BU trends in methane emissions are available for anthropogenic emissions using four global inventories (EDGARv6 and v7, CEDS, GAINS and EPA2019), five fire products for biomass burning (GFEDv4.1s, QFEDv2.5, GFAS and FINNv1.6 and v2.5) and 13 biogeochemical models for wetland emissions (Saunio *et al* 2024). However, estimates for other natural sources such as geological, termites, permafrost, rivers, lakes, and reservoirs available in the literature lack sufficient measurements to analyze temporal changes in methane emissions and, as a

result, trends cannot currently be calculated for these sources.

Estimated methane emissions from inland freshwaters for the new global methane budget use new spatial products and for the first time attribute some freshwater sources to anthropogenic activities ('direct' via river damming or other human-constructed small lakes and ponds) or influences ('indirect' via eutrophication induced by enhanced nutrient loadings from the surrounding catchments). Notable improvements over the last GMB include the addition of new, spatially explicit estimates of lake and reservoir emissions derived from both observations and models (Johnson *et al* 2021, 2022, Zhuang *et al* 2023).

To further interpret estimated methane emissions changes in recent years after the GMB budget period in 2020, we use a TD emission quantification based on methane column measurements from TROPOMI for the years 2018–2023. This inverse system is based on the GEOS-Chem adjoint 4D-Var methane inverse system (Yu *et al* 2021). Prior fluxes, treatments, and optimization configurations are as described in Yu *et al* (2021 and 2023). Results here are the average of two inversions: one uses a fixed OH field from chemical transport model simulations, whereas the other optimizes OH concentration magnitude simultaneously with methane emissions. To extend the evaluation period from the GMB model ensemble, the recent-year emission increases are based on the emission estimates of 2019 and 2023 from this model (GEOS-Chem) constrained by a TROPOMI product, rather than a comparison to the GMB year-2019 estimates.

2. Global sources and sinks of methane

Despite an increasing policy focus on methane as a potent greenhouse gas, methane emissions continue to rise. Global anthropogenic methane emissions reached 370 [range 343–403] and 384 [358–411] Tg CH₄ yr⁻¹ based on BU and TD estimates, respectively, averaged for the three years from 2018 to 2020 (table 1). These emissions are 50–60 Tg CH₄ yr⁻¹ (15%–20%) higher than for the period 2000–2002, nearly two-decades earlier (table 1). Total global methane sources, both natural and anthropogenic, rose by 50–70 Tg CH₄ yr⁻¹.

Our best estimates for anthropogenic methane emissions in 2020, the last year for which full data for the GMB are available, are 372 [345–409] and 392 [368–409] Tg CH₄ yr⁻¹ for BU and TD methods, respectively (figure 1, table 1). The largest emissions sources are: wetland and inland freshwaters, agriculture and waste, and fossil fuel production and use (figure 1). Direct anthropogenic emissions from TD estimates now comprise $\sim 65\%$ of global emissions. When the ~ 50 yr⁻¹ or more of 'indirect

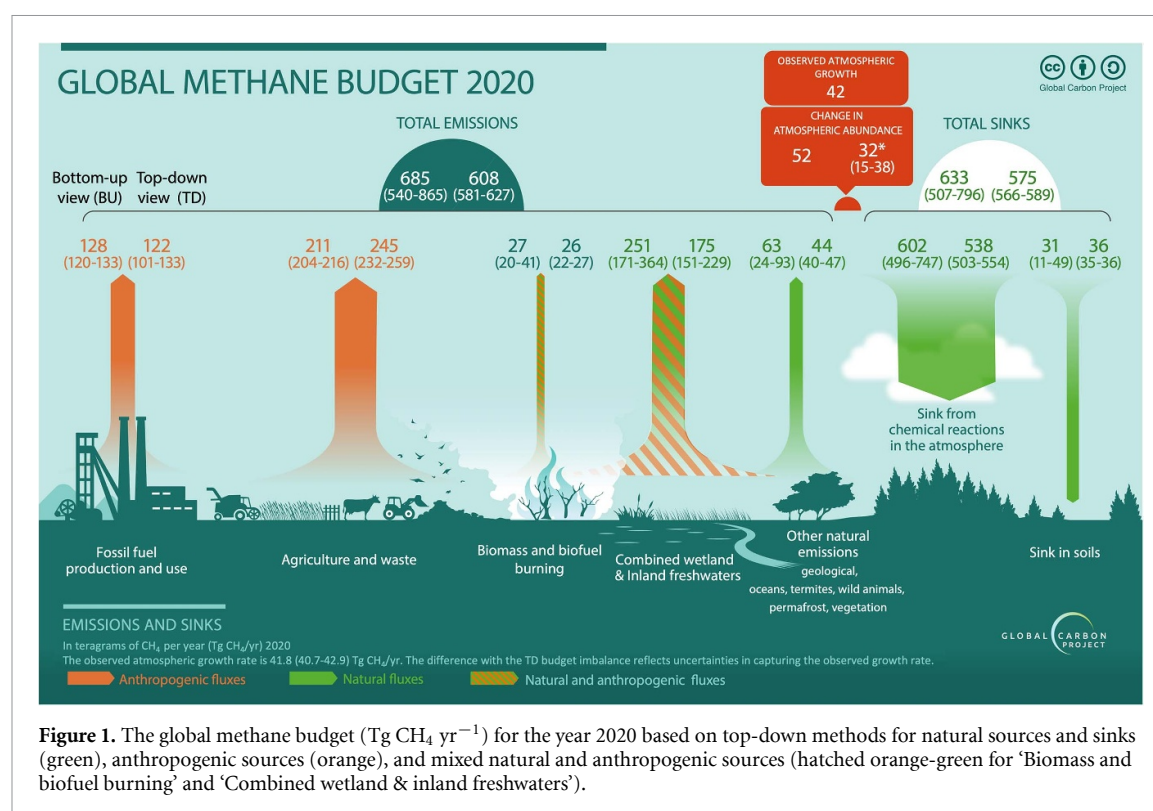
Table 1. Mean global methane emissions by source type in Tg CH₄ yr^{−1} for the period 2000–2002 (left columns), 2018–2020 (center columns) and 2020 (right columns) using bottom-up (BU) and top-down (TD) approaches. Because top-down models cannot fully separate individual processes, only five categories of emissions are provided (see Saunio *et al* 2024). Uncertainties are reported as [min–max] range of reported studies. Differences of 1 Tg CH₄ yr^{−1} in the totals can occur attributable to rounding errors. ‘Total chemical loss’ includes atmospheric loss from tropospheric OH and Cl as well as stratospheric loss.

Period of time	2000–2002		2018–2020		2020	
	BU	TD	BU	TD	BU	TD
NATURAL & INDIRECT ANTHROPOGENIC SOURCES						
All inland waters	242 [155–356]		251 [166–372]		251 [171–364]	175 [151–229]
Wetlands	153 [115–190]	170 [153–227]	162 [126–206]	169 [149–223]	161 [131–198]	175 [151–229]
Inland freshwaters	112 [49–202]		112 [49–202]		112 [49–202]	
Double counting	23 [9–36]		23 [9–36]		−23 [−9–−36]	
Other natural sources	63 [24–93]	45 [42–49]	63 [24–93]	43 [40–46]	63 [24–93]	44 [40–47]
Geological	35 [13–53]	23 [21–26]	35 [13–53]	22 [19–25]		
Termites	10 [4–16]	10 [10–12]	10 [4–16]	10 [9–11]		
Oceanic sources	13 [6–20]	12 [11–12]	13 [6–20]	12 [11–12]		
TOTAL NATURAL & INDIRECT SOURCES	305 [179–449]	211 [196–238]	314 [190–465]	210 [191–235]	314 [195–457]	216 [193–241]
DIRECT ANTHROPOGENIC SOURCES						
Agriculture and waste	186 [175–199]	206 [188–234]	219 [202–241]	239 [224–256]	211 [204–216]	245 [232–259]
Agriculture	129 [120–136]	139 [138–140]	147 [133–159]	159 [159–160]	147 [143–149]	
Enteric ferm. & manure	100 [95–107]	105 [104–106]	116 [108–122]	121 [120–122]	117 [114 – 124]	
Rice cultivation	29 [23–33]	34 [34–34]	32 [25–38]	38 [38–39]	32 [29–37]	
Landfills and waste	59 [50–68]	64 [62–64]	74 [59–83]	79 [72–82]	71 [60–84]	
Fossil fuels	96 [88–112]	101 [85–113]	123 [103–134]	119 [96–131]	128 [120–133]	122 [101–133]
Coal mining	25 [23–27]	25 [19–31]	41 [37–47]	35 [24–41]	41 [38–43]	
Oil & Gas	62 [57–69]	76 [63–88]	70 [53–79]	84 [73–95]	74 [67–80]	
Industry	4 [1–8]		5 [1–8]		5 [1–8]	
Transport	3 [1–7]		2 [1–3]		2 [1–3]	
Biomass & biofuel burning	26 [18–35]	25 [22–28]	28 [21–39]	26 [21–28]	27 [20–41]	26 [22–27]
Biomass burning	15 [10–21]	13 [11–16]	18 [14–25]	14 [10–16]	17 [13–27]	
Biofuel burning	11 [8–14]	11 [7–13]	11 [8–14]	12 [11–12]	10 [7–14]	
TOTAL DIRECT ANTHROPOGENIC SOURCES	309 [290–332]	333 [308–365]	370 [343–403]	384 [358–411]	372 [345–409]	392 [368–409]
TOTAL SOURCES	614 [469–781]	544 [517–587]	684 [533–868]	595 [569–609]	685 [540–865]	608 [581–627]

(Continued.)

Table 1. (Continued.)

SINKS					
Total chemical loss	503 [481–516]	537 [526–547]	602 [496–747]	538 [503–554]	
Tropospheric OH	474 [467–480]	505 [498–510]			
Stratospheric loss	27 [23–36]	28 [24–38]			
Tropospheric Cl	3 [0–8]	3 [0–9]			
Soil Uptake	34 [33–35]	36 [34–37]	31 [11–49]	36 [35–36]	
TOTAL SINKS	538 [529–549]	573 [562–582]	633 [507–796]	575 [566–589]	
IMBALANCE (SOURCES-SINKS)					
Total Sources	544 [517–587]	684 [533–868]	595 [569–609]	685 [540–865]	608 [581–627]
Total Sinks	538 [529–549]		573 [562–582]	633 [507–796]	575 [566–589]
Imbalance (Sources-Sinks)	6 [–12–38]		22 [6–26]	52	32 [15–38]
ATMOSPHERIC GROWTH					41.8 [40.7–42.9]



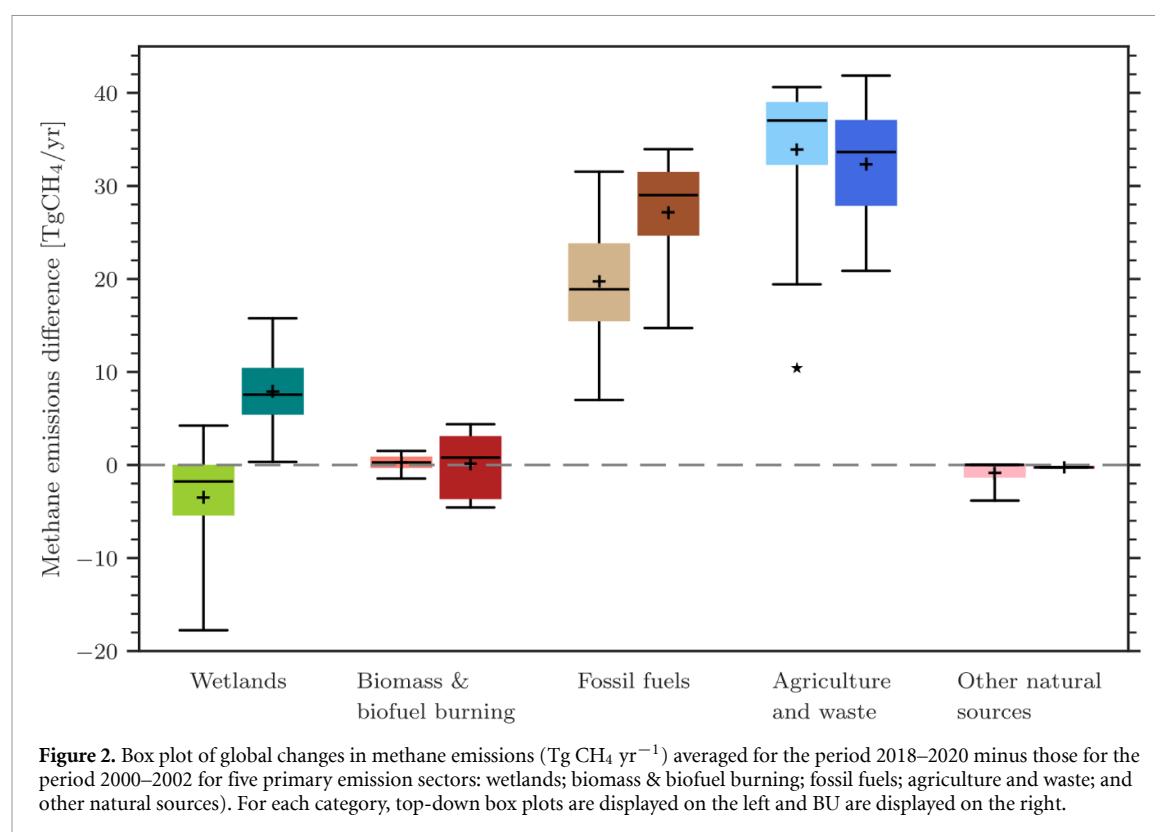
anthropogenic emissions,’ such as those from dams and reservoirs, are included (Saunois *et al* 2024), the total is more than two-thirds anthropogenic.

Almost all major sectors of anthropogenic emissions rose substantially from 2000 to 2020. Emissions from agriculture and waste rose by 33 Tg CH₄ yr⁻¹ or one-sixth overall to 219 and 239 Tg CH₄ yr⁻¹ for BU and TD estimates, respectively (figure 2, table 1). Emissions from cows (and other ruminants) and from landfills (and other waste) both rose by ~15 Tg CH₄ yr⁻¹ from 2000–2002 to 2018–2020. Fossil fuel emissions rose an estimated 18–27 Tg CH₄ yr⁻¹ (18%–28%) as estimated by TD and BU approaches, respectively (table 1). Methane emissions from fossil fuel extraction and use are now comparable to direct methane emissions from cows and other ruminants globally based on our estimate, but emissions from agriculture and waste, including landfills, remain approximately twice those associated with fossil fuels (table 1). This partitioning may vary among the individual inventories and TD estimates.

For natural emissions, inland freshwaters were estimated to emit 112 (49–202) Tg CH₄ yr⁻¹ globally. One major change from previous Global Methane Budgets is the allocation of some freshwater and wetland emissions to anthropogenic actions, such as emissions from human-built reservoirs (Saunois *et al* 2024). For example, 50% of inland water emissions (56 of 112 Tg yr⁻¹) are now estimated to be influenced by anthropogenic actions, including those from human-built reservoirs (30 Tg yr⁻¹) and through eutrophication, warming, and other

anthropogenically driven factors (Saunois *et al* 2024). Similarly, 30 Tg yr⁻¹ of the ~160 Tg yr⁻¹ emitted from wetlands globally (table 1) are estimated to be influenced by anthropogenic factors such as climate change and CO₂ fertilization. Given this new partitioning of previously categorized ‘natural’ wetland and inland freshwater emissions, the contribution of ‘anthropogenic methane emissions’ is likely to be greater than two-thirds, even when including only the additional 30 Tg yr⁻¹ of emissions from human-built reservoirs.

The indirect (non-reservoir) anthropogenic emissions, however, need follow-up investigations using process-based models similar to those used to perform regional (e.g. Guo *et al* 2020) or global (e.g. Zhuang *et al* 2023) assessments of future emissions under future climate scenarios. Such models consistently project a substantial increase in methane emissions by the end of the 21st century (in the range of about 30%–80% depending on the scenario), supporting the notion that—like wetlands—inland freshwaters are also sensitive to warming. This feedback is poorly accounted for in the current decomposition between present-day natural and anthropogenic component fluxes and eutrophication. Such increases, whether induced by direct or indirect (climate change, eutrophication) drivers, have likely already contributed to the observed decadal increase in atmospheric CH₄ concentrations. Their contribution remains relatively unquantified, however, contributing to uncertainties in the assessment of decadal changes in the GMB.



Natural wetlands showed no statistically significant increase in methane emissions when comparing the three-year periods 2000–2002 to 2018–2020 (table 1).

Global methane sinks are increasing in response to rising atmospheric methane concentrations. Total global sinks estimated by TD approaches rose by $35 \text{ Tg CH}_4 \text{ yr}^{-1}$ from an average $538 [529\text{--}549] \text{ Tg CH}_4 \text{ yr}^{-1}$ in 2000–2002 to $573 \text{ Tg CH}_4 \text{ yr}^{-1}$ for the period 2018–2020 (table 1). Unsurprisingly, most of the increased oxidation of methane ($\sim 30 \text{ Tg CH}_4 \text{ yr}^{-1}$) came from OH radicals in the troposphere.

The imbalance between global sources and sinks continues to grow and is reflected in the increasing atmospheric growth rates observed for methane in recent years (Lan *et al* 2024). The average imbalance between global sources and sinks in the early 2000s was $\sim 6 \text{ Tg CH}_4 \text{ yr}^{-1}$ (table 1). In contrast, this imbalance grew to $32 [15\text{--}38]$ and $52 \text{ Tg CH}_4 \text{ yr}^{-1}$ in 2020 based on TD and BU methods, respectively, values that bracket the actual atmospheric growth rate of 15 ppb CH_4 or 42 Tg CH_4 that year (Lan *et al* 2024).

3. Regional and latitudinal methane sources and sinks

The estimated global increase in methane emissions from 2000 to 2020 arises largely from four

regions or countries (figure 3, table 2): China (BU: $19 [17\text{--}23] \text{ Tg CH}_4 \text{ yr}^{-1}$; TD: $7 [-7\text{--}17] \text{ Tg CH}_4 \text{ yr}^{-1}$), South Asia (BU: $10 [7\text{--}14] \text{ Tg CH}_4 \text{ yr}^{-1}$; TD: $10 [2\text{--}17] \text{ Tg CH}_4 \text{ yr}^{-1}$), SouthEast Asia (BU: $8 [0\text{--}14] \text{ Tg CH}_4 \text{ yr}^{-1}$; TD: $6 [-2\text{--}10] \text{ Tg CH}_4 \text{ yr}^{-1}$) and the Middle East (BU: $8 [4\text{--}15] \text{ Tg CH}_4 \text{ yr}^{-1}$; TD: $8 [2\text{--}22] \text{ Tg CH}_4 \text{ yr}^{-1}$), mostly attributable to anthropogenic emissions. These regions are followed by Equatorial Africa (BU: $7 [3\text{--}17] \text{ Tg CH}_4 \text{ yr}^{-1}$; TD: $4 [-2\text{--}8] \text{ Tg CH}_4 \text{ yr}^{-1}$) and the USA (BU: $3 [-3\text{--}18] \text{ Tg CH}_4 \text{ yr}^{-1}$; TD: $6 [-6\text{--}16] \text{ Tg CH}_4 \text{ yr}^{-1}$). However, large uncertainties exist among each approach, and discrepancies appear between approaches for China, the USA and Equatorial Africa. Two groups of countries show decreasing emissions: Europe (BU: $-7 [-10\text{--}4] \text{ Tg CH}_4 \text{ yr}^{-1}$; TD: $-7 [-10\text{--}2] \text{ Tg CH}_4 \text{ yr}^{-1}$) as highlighted previously (Jackson *et al* 2020) and, possibly, Australasia (BU: $-1 [-4\text{--}2] \text{ Tg CH}_4 \text{ yr}^{-1}$; TD: $0 [-2\text{--}0] \text{ Tg CH}_4 \text{ yr}^{-1}$).

The distribution of emission changes from 2000 to 2020 by latitude emphasizes the tropics, which contribute an estimated $\sim 60\%\text{--}70\%$ of the total global change over the last two decades for both approaches (BU: $45 [29\text{--}68] \text{ Tg CH}_4 \text{ yr}^{-1}$; TD: $36 [6\text{--}47] \text{ Tg CH}_4 \text{ yr}^{-1}$) (table 2). Mid-latitudes are responsible for the additional $30\%\text{--}40\%$ increase in global emissions; in contrast, emissions from higher latitudes ($60\text{--}90^\circ\text{N}$) are estimated to be stable or to have decreased slightly, attributable to slightly decreasing anthropogenic emissions (table 2).

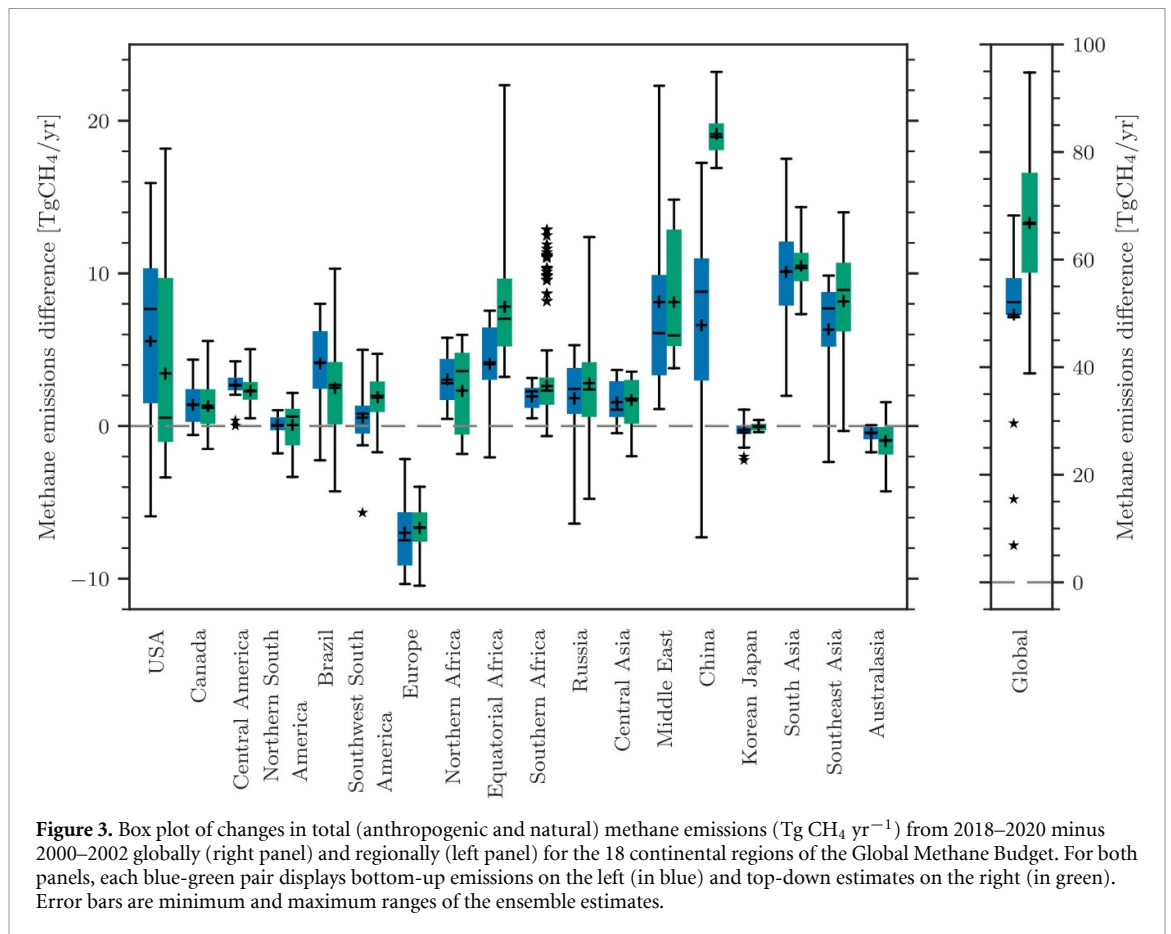
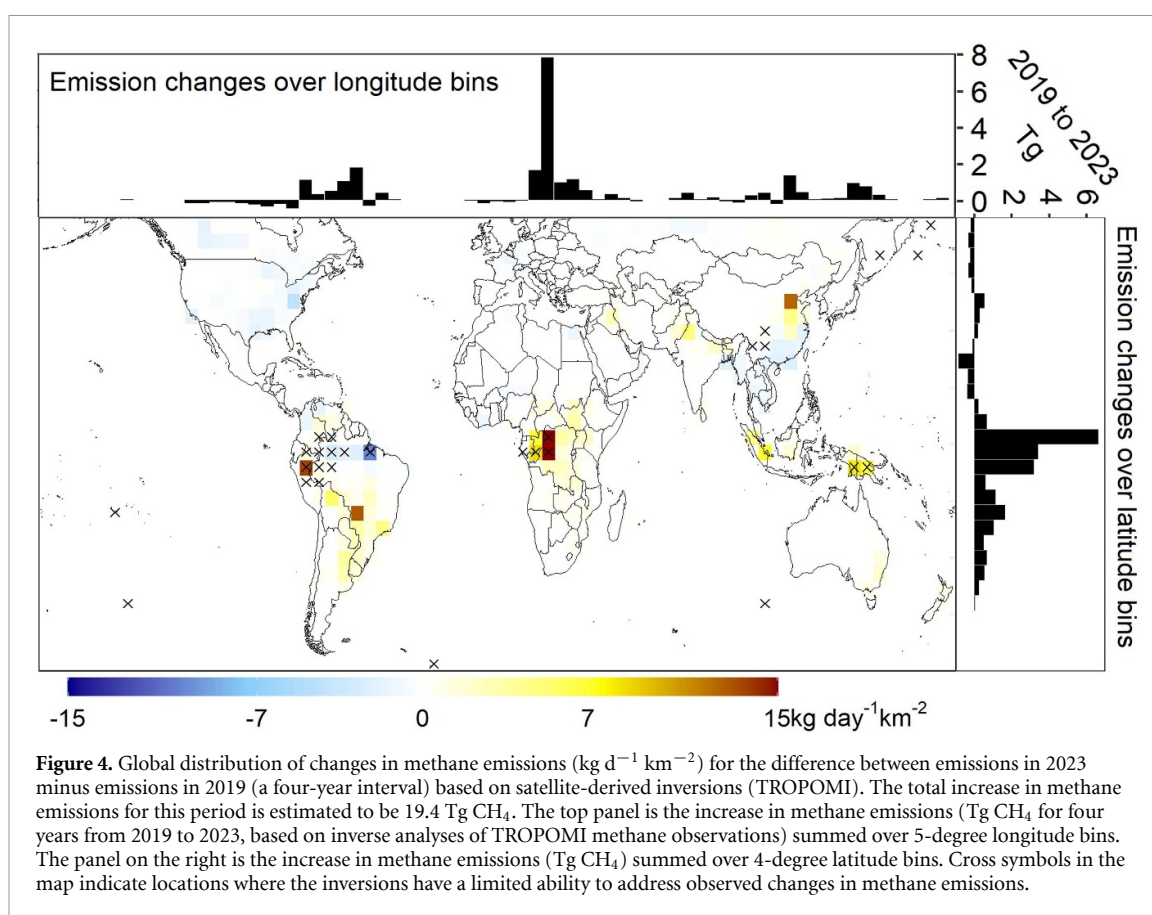


Table 2. Global, latitudinal and regional changes in $\text{Tg CH}_4 \text{ yr}^{-1}$ averaged for the period 2018–2020 minus 2000–2002 for bottom up (BU) and top-down (TD) methods. The latitudinal estimates are based on gridded datasets resulting in a slight discrepancy with the global total for the BU approaches. Outlier detection and removal is performed for each source category and region, leading to small discrepancies when adding categories and latitudinal bands or regions together.

	Natural and indirect anthropogenic emissions		Direct anthropogenic emissions		Total sources	
	BU	TD	BU	TD	BU	TD
Global	8 [0–16]	−4 [−18–2]	59 [39–79]	54 [25–69]	67 [39–95]	56 [49–68]
90N–60N	1 [−2–3]	0 [−1–1]	−4 [−7–1]	−1 [−5–1]	−3 [−9–3]	−1 [−6–1]
60N–30N	3 [−2–7]	−1 [−6–4]	27 [21–34]	16 [8–26]	30 [20–40]	15 [5–25]
−90S–30N	4 [−2–17]	−4 [−14–4]	41 [31–51]	41 [30–48]	45 [29–68]	36 [6–47]
USA	2 [0–6]	0 [0–0]	1 [−4–12]	5 [−5–13]	3 [−3–18]	6 [−6–16]
Canada	0 [−1–3]	0 [−2–1]	1 [−1–3]	1 [0–3]	1 [−2–6]	1 [−1–4]
Central America	0 [0–2]	0 [0–0]	2 [1–3]	3 [1–5]	2 [0–5]	3 [2–4]
Northern South America	0 [0–1]	0 [−1–1]	0 [−3–1]	0 [0–1]	0 [−3–2]	0 [−2–1]
Brazil	0 [−3–5]	−1 [−5–2]	2 [−1–5]	5 [3–7]	2 [−4–10]	4 [−2–8]
Southwest South America	0 [−2–2]	−1 [−6–3]	2 [1–2]	2 [0–3]	2 [−2–5]	1 [−1–5]
Europe	0 [−2–1]	0 [−1–0]	−6 [−8–5]	−7 [−9–2]	−7 [−10–4]	−7 [−10–2]
Northern Africa	0 [0–1]	0 [−1–0]	2 [−2–5]	3 [1–5]	2 [−2–6]	3 [0–6]
Equatorial Africa	1 [−1–4]	0 [−2–2]	6 [4–13]	4 [0–6]	7 [3–17]	4 [−2–8]
Southern Africa	0 [0–0]	0 [−1–1]	2 [0–5]	2 [1–3]	2 [−1–5]	2 [0–3]
Russia	1 [0–3]	0 [−2–1]	2 [−1–10]	2 [−5–5]	3 [−1–12]	2 [−6–5]
Central Asia	0 [0–0]	0 [0–0]	2 [0–3]	2 [0–4]	2 [0–4]	2 [1–4]
Middle East	0 [0–0]	0 [−1–0]	8 [4–15]	8 [2–22]	8 [4–15]	8 [2–22]
China	1 [0–2]	0 [0–0]	18 [17–21]	7 [−8–17]	19 [17–23]	7 [−7–17]
Korean Japan	0 [0–0]	0 [0–0]	0 [0–0]	0 [−2–1]	0 [0–0]	0 [−1–1]
South Asia	1 [−1–4]	0 [−1–0]	10 [9–11]	10 [3–18]	10 [7–14]	10 [2–17]
SouthEast Asia	0 [−2–2]	−1 [−7–0]	8 [1–12]	8 [2–12]	8 [0–14]	6 [−2–10]
Australasia	0 [−1–0]	−1 [−1–1]	0 [−2–1]	0 [−1–0]	−1 [−4–2]	0 [−2–0]



4. More recent emission estimates (2019–2023)

Extending emission estimates into the year 2023 based on TD analyses of TROPOMI satellite measurements, estimated global methane emissions increase by an additional 19 Tg over the 4 year interval from 2019 to 2023 (figure 4). Tropical regions contribute the most to recent emission increases (>7 Tg from 2019 to 2023), particularly in the Congo and, to a lesser extent, parts of southeast Asia and southern Brazil (figure 4). Another area of increase from 2019 to 2023 is observed near Beijing, China (figure 4). As a full ensemble of inversions becomes available with more data through 2023, additional estimates will provide more comprehensive coverage of emission increases.

5. Conclusions

Methane is receiving increasing policy attention because of its potential for reducing warming over the next few decades. Recent analyses suggest that methane mitigation may be cheaper than CO_2 mitigation for a comparable climate benefit (UNEP & CCAC 2021). Better quantification and attribution of methane sources are needed to support such mitigation efforts locally, regionally, and globally.

Closer-to-real-time estimates of methane sources, for example, will be aided by new satellites such

as MethaneSAT and CarbonMapper, to identify and quantify methane super-emitters (Duren *et al* 2019). Current BU inventories do a poor job of representing the long tail of such emissions in inventory budgets. More complete (and rapid) incorporation of satellite data will also improve TD methane inversions, regional emission estimates, and national greenhouse gas inventories. As part of upcoming GMB efforts, we expect to produce national methane budgets for some key countries.

Uncertainties in methane emissions remain even greater for natural sources, such as wetlands, freshwater systems, and natural geologic sources. Process-based model assessments of inland freshwater CH_4 emissions are needed that rely on common system delineations and simulation protocols. This effort could follow a format similar to that of the WETland CH_4 Inter-comparison of Models Project (WETCHIMP) launched a decade or more ago (Melton *et al* 2013). Process-based models are needed to constrain uncertainties, to strengthen confidence in the spatial upscaling of CH_4 fluxes, and to resolve temporal variability (e.g. responses to climate extremes, inter-annual variations, and decadal trends). Similar to past wetland studies, simulations should be performed within the broader framework of land-surface models (LSMs) and would benefit from recent advances in LSM-based simulations of inland water CO_2 and N_2O fluxes (e.g. Yao *et al* 2020, Zhang *et al* 2022, Tian *et al* 2023).

TD inversions will benefit from incorporating additional tracers, including ethane and $^{13}\text{CH}_4$ —wherever global data are available—to enhance CH_4 abundance data from flask and satellite sampling. Ethane, for instance, and methane are co-emitted from fossil fuel exploration, but not from biological sources (e.g. Lan *et al* 2019, Barkley *et al* 2021). Additionally, methane produced from biological processes, such as in wetlands, landfills, or livestock, typically has a lighter $^{13}\text{CH}_4$: $^{12}\text{CH}_4$ ratio compared to methane from fossil fuel extraction or industrial processes. Different sinks also fractionate against the slightly heavier $^{13}\text{CH}_4$ consuming it at a slightly slower rate than for $^{12}\text{CH}_4$. Incorporating these additional tracer measurements can thus help researchers identify and quantify the contributions of methane sources and sinks more accurately. Furthermore, TD quantification would benefit from the recent advances in synthesizing $^{13}\text{CH}_4$ source signatures into grid-level estimates for fossil and non-fossil sources (Sherwood *et al* 2021).

Estimates of methane sinks also require new approaches and research tools. The oxidative capacity of the atmosphere is difficult to measure directly, particularly for short-lived OH and Cl radicals that oxidize most emitted methane. Methyl chloroform (CH_3CCl_3) has provided the most useful constraint on the atmosphere's oxidative capacity (Patra *et al* 2021). However, its abundance has been declining for decades and is now below 1 pptv (Rigby *et al* 2017). We need new tracers and tools to assess the abundance of OH radicals, in particular, which have a lifetime of only seconds. Opportunities to constraint the oxidative capacity of the troposphere include other halogens compounds such as HFC-134a, HFC-32 and HCFC-141b (Thompson *et al* 2024) and isotopic information from ^{14}CO (Brenninkmeijer 1993) and ^{13}CO (Mak and Brenninkmeijer 1998).

Methane concentrations have risen faster over the past five-year period than in any period since record-keeping began. Understanding where and why this is happening is a central goal of the Global Methane Budget. At least two-thirds of global methane emissions are now attributable to anthropogenic sources, an outcome that cannot continue if we are to maintain a habitable climate.

Data availability statement

The data that support the findings of this study are openly available at the following URL/DOI: <https://www.icos-cp.eu/GCP-CH4-2024>.

Acknowledgments

The authors acknowledge the many scientists who contribute to the Global Methane Budget released by the Global Carbon Project (globalcarbonproject.org). Our research was supported by

the Gordon and Betty Moore Foundation through Grants GBMF5439 'Advancing Understanding of the Global Methane Cycle' and GBMF11519 'Advancing the understanding of methane emissions from tropical wetlands' to Stanford University and the Agence National de la Recherche through the project Advanced Methane Budget through Multi-constraints and Multi-data streams Modelling (AMB-M³)—(ANR-21-CE01-0030). The authors acknowledge additional funding through the framework of UNEP's International Methane Emissions Observatory (IMEO) (#DTIE21-EN3143 to Stanford University, the Laboratoire des Sciences du Climat et de l'Environnement (LSCE-IPSL), and CSIRO Environment, Canberra, Australia) and from Australia's National Environmental Science Program - Climate Systems Hub (JGC) and from Future Earth. PRE acknowledges funding from the FRS-FRNS PDR project T.0191.23 CH4-lakes.

ORCID iDs

R B Jackson  <https://orcid.org/0000-0001-8846-7147>

M Saunio  <https://orcid.org/0000-0003-3983-2931>


A Martinez  <https://orcid.org/0000-0001-8508-9005>

J G Canadell  <https://orcid.org/0000-0002-8788-3218>

X Yu  <https://orcid.org/0000-0002-9380-5136>

M Li  <https://orcid.org/0000-0003-0620-6301>

B Poulter  <https://orcid.org/0000-0002-9493-8600>

P A Raymond  <https://orcid.org/0000-0002-8564-7860>

P Regnier  <https://orcid.org/0000-0002-4531-0868>

P Ciais  <https://orcid.org/0000-0001-8560-4943>

S J Davis  <https://orcid.org/0000-0002-9338-0844>

P K Patra  <https://orcid.org/0000-0001-5700-9389>

References

- Barkley Z R *et al* 2021 Analysis of oil and gas ethane and methane emissions in the Southcentral and Eastern United States using four seasons of continuous aircraft ethane measurements *J. Geophys. Res. Atmos.* **126** e2020JD034194
- Brenninkmeijer C A M 1993 Measurement of the abundance of ^{14}CO in the atmosphere and the $^{13}\text{C}/^{12}\text{C}$ and $^{18}\text{O}/^{16}\text{O}$ ratio of atmospheric CO with applications in New Zealand and Antarctica *J. Geophys. Res.* **98** 10595–614
- Duren R M *et al* 2019 California's methane super-emitters *Nature* **575** 180–4
- Forster P *et al* 2021 The Earth's energy budget, climate feedbacks, and climate sensitivity *Climate Change 2021: The Physical Science Basis. Contribution of Working Group I to the Sixth Assessment Report of the Intergovernmental Panel on Climate Change* ed V Masson-Delmotte *et al* (Cambridge University Press)
- Guo M, Zhuang Q, Tan Z, Shurpali N, Juutinen S, Kortelainen P and Martikainen P J 2020 Rising methane emissions from boreal lakes due to increasing ice-free days *Environ. Res. Lett.* **15** 064008

- IPCC 2021 Summary for policymakers *Climate Change 2021: The Physical Science Basis. Contribution of Working Group I to the Sixth Assessment Report of the Intergovernmental Panel on Climate Change* ed V Masson-Delmotte *et al*
- Jackson R B, Saunois M, Bousquet P, Canadell J G, Poulter B, Stavert A R, Bergamaschi P, Niwa Y, Segers A and Tsuruta A 2020 Increasing anthropogenic methane emissions arise equally from agricultural and fossil fuel sources *Environ. Res. Lett.* **15** 071002
- Johnson M S, Matthews E, Bastviken D, Deemer B, Du J and Genovese V 2021 Spatiotemporal methane emission from global reservoirs *J. Geophys. Res.* **126** e2021JG006305
- Johnson M S, Matthews E, Du J, Genovese V and Bastviken D 2022 Methane emission from global lakes: new spatiotemporal data and observation-driven modeling of methane dynamics indicates lower emissions *J. Geophys. Res.* **127** e2022JG006793
- Lan X *et al* 2019 Long-term measurements show little evidence for large increases in total U.S. methane emissions over the past decade *Geophys. Res. Lett.* **46** 4991–9
- Lan X, Thoning K W and Dlugokencky E J 2024 Trends in globally-averaged CH₄, N₂O, and SF₆ determined from NOAA global monitoring laboratory measurements Online: Version 2024–06 (<https://doi.org/10.15138/P8XG-AA10>)
- Mak J E and Brenninkmeijer C A M 1998 Measurement of ¹³C and C¹⁸O in the free troposphere *JGR Atmos.* **103** 19347–58
- Melton J R *et al* 2013 Present state of global wetland extent and wetland methane modelling: conclusions from a model inter-comparison project (WETCHIMP) *Biogeosciences* **10** 753–88
- NRC 2023 Natural resources canada canadian interagency forest fire center *National Fire Situation Report*
- Patra P K *et al* 2021 Methyl chloroform continues to constrain the hydroxyl (OH) variability in the troposphere *J. Geophys. Res. Atmos.* **126** e2020JD033862
- Peng S *et al* 2022 Wetland emission and atmospheric sink changes explain methane growth in 2020 *Nature* **612** 477–82
- Rigby M *et al* 2017 Role of atmospheric oxidation in recent methane growth *Proc. Natl Acad. Sci. USA* **114** 5373–7
- Rodrigues M 2023 The Amazon's record-setting drought: how bad will it be? *Nature* **623** 675–6
- Saunois M *et al* 2016 The global methane budget 2000–2012 *Earth Syst. Sci. Data* **8** 697–751
- Saunois M *et al* 2020 The global methane budget 2000–2017 *Earth Syst. Sci. Data* **12** 1561–623
- Saunois M *et al* 2024 Global methane budget 2000–2020 *Earth Syst. Sci. Data* submitted (<https://doi.org/10.5194/essd-2024-115>)
- Sherwood O A, Schwietzke S and Lan X 2021 Global inventory of fossil and N=non-fossil $\delta^{13}\text{C}$ -CH₄ source signature measurements for improved atmospheric Modeling (NOAA Global Monitoring Laboratory Data Repository [data set]) p 10
- Skeie R B, Hodnebrog Ø and Myhre G 2023 Trends in atmospheric methane concentrations since 1990 were driven and modified by anthropogenic emissions *Commun. Earth Environ.* **4** 1–14
- Thompson R L *et al* 2024 Estimation of the atmospheric hydroxyl radical oxidative capacity using multiple hydrofluoro-carbons (HFCs) *Atmos. Chem. Phys.* **24** 1415–27
- Tian H *et al* 2023 Increased terrestrial carbon export and CO₂ evasion from global Inland waters since the preindustrial era *Glob. Biogeochem. Cycles* **37** e2023GB007776
- United Nations Environment Programme and Climate and Clean Air Coalition 2021 *Global Methane Assessment: Benefits and Costs of Mitigating Methane Emissions* (United Nations Environment Programme)
- WMO 2024 *The State of the Global Climate 2023*
- Yao Y, Tian H, Shi H, Pan S, Xu R, Pan N and Canadell J G 2020 Increased global nitrous oxide emissions from streams and rivers in the anthropocene *Nat. Clim. Change* **10** 138–42
- Yu X, Millet D B and Henze D K 2021 How well can inverse analyses of high-resolution satellite data resolve heterogeneous methane fluxes? Observing system simulation experiments with the GEOS-Chem adjoint model (v35) *Geosci. Model Dev.* **14** 7775–93
- Yu X, Millet D B, Henze D K, Turner A J, Delgado A L, Bloom A A and Sheng J 2023 A high-resolution satellite-based map of global methane emissions reveals missing wetland, fossil fuel, and monsoon sources *Atmos. Chem. Phys.* **23** 3325–46
- Zhang H, Lauerwald R, Ciais P, Van Oost K, Guenet B and Regnier P 2022 Global changes alter the amount and composition of land carbon deliveries to European rivers and seas *Commun. Earth Environ.* **3** 1–11
- Zhao Y *et al* 2020 Influences of hydroxyl radicals (OH) on top-down estimates of the global and regional methane budgets *Atmos. Chem. Phys.* **20** 9525–46
- Zhuang Q, Guo M, Melack J M, Lan X, Tan Z, Oh Y and Leung L R 2023 Current and future global lake methane emissions: a process-based modeling analysis *J. Geophys. Res.* **128** e2022JG007137